

Shape Memory Alloys and their Thermal Characteristics

R. Sundara Raman

Assistant Professor, Department of Mechanical Engineering, Indian Naval Academy, Kannur, Kerala, India
 E-Mail: sundararaman792@gmail.com

Abstract - The smart structures are sometimes called “intelligent” or “adaptive” structures, being a class of advanced structures having highly distributed actuators and sensors combined with structural functionality, distributed control functions and even computing architectures. The structures are able to vary their geometric configurations as well as their physical characteristics subject to control laws. These include piezoelectric, electrostrictives, magnetostrictives, ionic polymers, Shape Memory Alloys (SMA), and magnetic shape memory alloys (MSMAs). Development of smart structures involves the integration of active and passive material systems, often including the coupling of relevant mechanical, electrical, magnetic, thermal, or other physical properties. This can subject the active materials to large stress levels, cyclic loads, thermal loads, or environmental loads that result in non-linear responses and large variations in material properties. Smart materials are not only singular materials; rather, they are also hybrid composites or integrated systems of materials. Shape memory alloys (SMAs) are one of the major elements of smart hybrid composites because of their unique properties, such as shape memory effect, pseudo elasticity and high damping capacity. These properties in smart hybrid composites provide tremendous potential for creating new paradigms for material - structural interactions and demonstrate various successes in many engineering applications, such as vibration control, actuators in MEMS, and a variety of others.

Keywords: Shape Memory Alloys (SMA), Ionic Polymers, Hybrid Composites, Non-Linear Responses, Intelligent/ Adaptive Structures, Elastomers

I. INTRODUCTION

Structures that can actively adapt to changing environmental conditions are becoming a reality. These “smart” structures are being developed for a variety of military and commercial applications. For example, the DARPA/McDonnell Douglas and DARPA/Boeing are using smart materials to improve the performance of helicopter rotor blades. These smart materials actively control the shape of the rotor blades through actuation of trailing edge trim tabs, edge flaps, and passive torque tubes in order to reduce vibrations and improve lift. When large changes in shape are controlled, actuators fabricated with Shape Memory Alloys (SMAs) are used. These active structures take advantage of the unique thermo mechanical behavior of SMAs, known as the Shape Memory Effect (Fig. 1), which results in large, recoverable deformations when the alloys are heated. The resulting power ratios are very high, which enable SMA actuated systems to be fabricated at much smaller size scales than conventional hydraulic or mechanical actuation systems. The SMA devices used in

these structures are constructed from wires and tubes that are “trained” to actuate the structure. The high power ratio of SMAs has been especially beneficial in designing and developing actuators for controlling robotic hands. SMAs possess many other characteristics that are desirable for actuation applications. For example, actuators can be fabricated from a single SMA element, resulting in simpler and more reliable devices. SMA actuators made from Ni-Ti are highly corrosion resistant, and with no additional vibrating parts they are silent, clean, and relatively unaffected by the operating environment. Smooth movements can also be achieved with these actuators, making them ideally suited for spacecraft. New opportunities for expanding the use of SMAs in the design of smart structure are being realized by embedding NiTi wires into polymers, elastomers, and fiber-reinforced/epoxy composites. The embedded wires can be used to activate flexible materials, like polymers and elastomers, or improve the toughness and buckling resistance of brittle materials, like fiber-reinforced/epoxy composites.

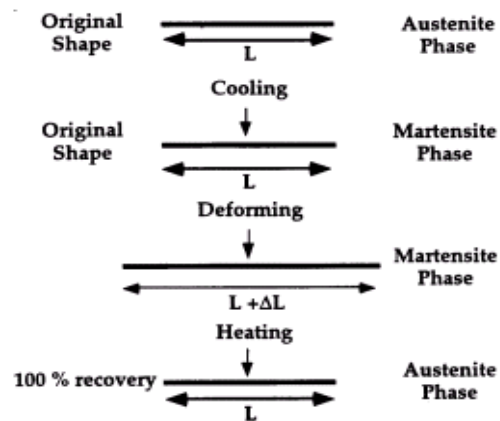


Fig. 1 Schematic illustrating the Shape Memory Effect

II. MECHANICAL BEHAVIOR OF SHAPE MEMORY ALLOYS

The mechanical behavior of SMAs is characterized by phase transformations that are activated through changes in temperature and/or loading. These transformation lead to very large recoverable deformations, otherwise known as the Shape Memory Effect or pseudo elasticity (Fig. 2). Three-dimensional T-s-e diagrams are often constructed to describe this behavior for design purposes. However, these diagrams can only be used to predict the cooling behavior of

isobaric ally loaded structures; therefore they may not be useful in predicting their behavior under complex loading and temperature paths. To account for the complex thermo mechanical constitutive behavior of SMAs, some general models have been proposed.

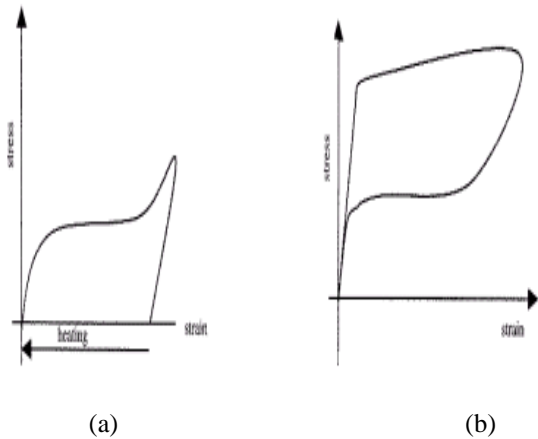


Fig. 2 (a) Shape Memory Effect at $T < A_s$ and (b) Pseudo elasticity at $T > A_f$ for a SMA

The shape memory effect is observed when the temperature of a piece of shape memory alloy is cooled to below the temperature M_f . At this stage the alloy is completely composed of Martensite which can be easily deformed. After distorting the SMA the original shape can be recovered simply by heating the wire above the temperature A_f . The heat transferred to the wire is the power driving the molecular rearrangement of the alloy, similar to heat melting ice into water, but the alloy remains solid. The deformed Martensite is now transformed to the cubic Austenite phase, which is configured in the original shape of the wire.

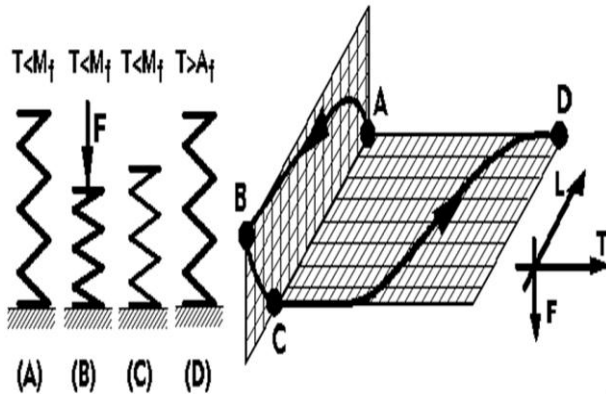


Fig. 3 The one way memory effect. The sample is deformed (A to B) and unloaded (B to C) at a temperature below M_f . The residual deformation is restored during heating to a temperature above A_f

Pseudo-elasticity occurs in shape memory alloys when the alloy is completely composed of Austenite (temperature is greater than A_f). Unlike the shape memory effect, pseudo-elasticity occurs without a change in temperature. The load on the shape memory alloy is increased until the Austenite becomes transformed into Martensite simply due to the loading; this process is shown in Figure 2. The loading is

absorbed by the softer Martensite, but as soon as the loading is decreased the Martensite begins to transform back to Austenite since the temperature of the wire is still above A_f , and the wire springs back to its original shape.

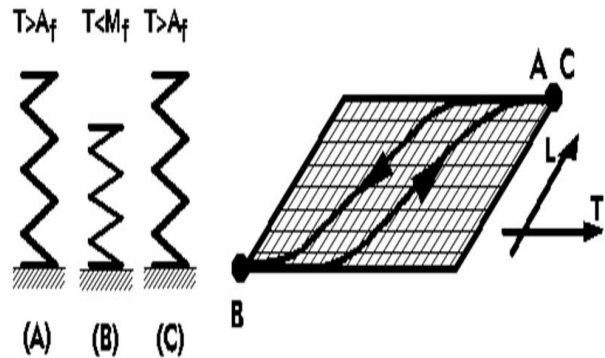


Fig. 4 The two way memory effect, A spontaneous shape change occurs during cooling to a temperature below M_f (A to B). This shape change is recovered during subsequent heating to a temperature above A_f (B to C)

III. SMA COMPOSITES

While comparisons of constitutive models for SMAs have been undertaken for designing smart structures using FEA, similar comparative analyses have not been performed for SMA composites. Micro-mechanical models have been proposed to quantify the effects of the shape and volume fraction of reinforcement on the thermo mechanical behavior of SMA composites using Mori-Tanaka's mean field and Eshelby's equivalent inclusion methods. However, because these models rely on the constitutive models for homogeneous SMAs, they can become far more computationally inefficient to use. Computational efficiency is especially important when considering the design of smart structures using SMA composites. Therefore, the use of simple constitutive models is imperative.

IV. SUPERELASTICITY OF SMA'S

Super elasticity is one of the most attractive properties of SMA's. It implies the attainment of very large strains (at least one order of magnitude greater than common metals) without any residual deformation upon unloading, while dissipating a considerable amount of energy. Fig. 1 shows a schematic stress-strain cyclic curve of a superelastic SMA. It is characterized by <ve branches. Branches 1 and 4 correspond to the elastic deformation of the two stable phases of SMA, respectively, austenite and martensite. Branches 2 and 3 correspond, respectively, to the forward (from austenite to detwinned martensite) and inverse (from detwinned martensite to austenite) phase transformation. Branch 5 corresponds to the onset of plastic deformation of detwinned martensite. The mechanical behavior of superelastic SMA's suits the optimal requirements of a seismic control device. Indeed, they could provide the device with (i) energy dissipation capability, to reduce acceleration and displacements caused by earthquakes, (ii) self-centering capability, to bring back the structure to its initial position when earthquake is over, (iii) good control of

the force transmitted by the device to the structure, (iv) high initial stiffness, to limit displacements under service actions or moderate earthquakes. Moreover, a seismic SMA based device stiffens in case of unpredicted strong actions (branch 4), thus assuring a good control of displacements even under unforeseen strong earthquakes.

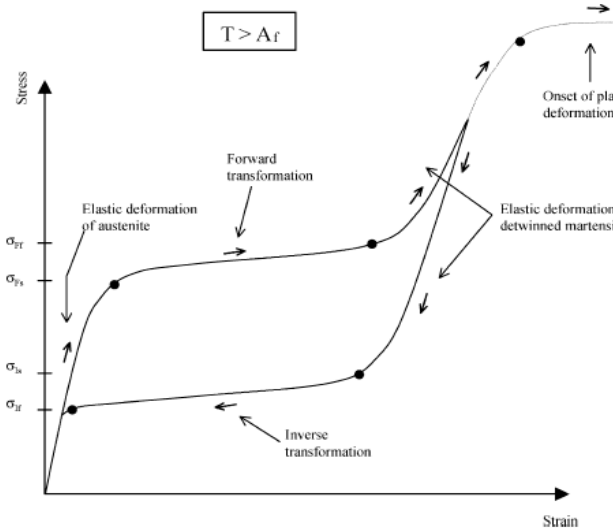


Fig. 5 Schematic stress–strain curve of superelastic shape memory alloy, showing the phenomena associated with the deformation process

Although the use of superelastic SMA’s appears to be very appealing under different points of view, some aspects have to be carefully examined:

1. The properties and the mechanical behavior of SMA’s strongly depend on alloy composition and thermo mechanical treatment.
2. Super elasticity is highly sensitive to temperature:
3. All SMA’s are superelastic only at some temperatures, i.e. between A_f and M_d to be useful in civil engineering applications, the superelastic range must be as wide as possible and must be centered around the average service temperature.
4. The transformation critical stresses increase linearly while increasing the temperature, with growth rate ranging from 3 up to 20 MPa/°C [12].
5. Although it is said that super elasticity is an isothermal phenomenon, this is practically not true because of the latent heat of transformation which causes the self-heating of the material. As the strain rate increases, the self-heating becomes significant, causing a rise of some degrees of the internal temperature. This yields modifications in the shape of the hysteresis loops, such as an apparent hardening of the plateau relevant to the phase transformations.
6. The mechanical behavior of SMA’s changes with repeated cyclic deformations.

V. FABRICATION AND TESTING OF SMA COMPOSITES

Model SMA composite specimens were fabricated by embedding untrained NiTi wires with diameters of 15 mils

into a woven fiberglass matrix. This matrix was then infiltrated with a compliant adhesive to increase the flexibility of the composite and improve the toughness of the matrix. The composite was then pressed between platens and cured at 80 C for 1 hour. Specimens contained 3, 6, and 9 embedded wires resulting in volume fractions of 0.081, 0.125, and 0.166. Dog-bone geometry was used for tensile testing, with a gage length of 1.5 inches and a width of 0.25 inches. Specimens were tested in an Instron screw-driven load frame at a displacement rate of 0.05 cm/min, resulting in an equivalent strain rate of 0.0002/sec. The specimens were aligned so that the direction of the fibers coincided with the loading direction for the specimen.

VI. RESULTS

Experimental results from testing 3, 6 and 9 wire SMA composites and plain fiberglass specimens can be seen in Fig. 6. The mechanical behavior of the composites was reasonably reproducible Fig. 7. It is immediately evident that the composites exhibit greater ductility than either the composite or fiberglass specimens. By increasing ductility, composites provide the basis for fabricating more flexible smart structures with larger actuation strokes. However, this enhanced ductility is obtained at the expense of strength. While the ductility of the composites is 100% greater than the wire and nearly 600% greater than the fiberglass, the ultimate strength is almost identical to the fiberglass composite and about 20% of the wire. The mechanical behavior of the composites exhibited slight variations with composition, with the strength and ductility increasing in conjunction with the wire reinforcement.

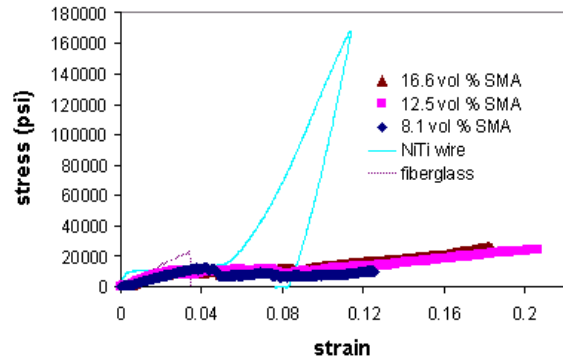


Fig. 6 Uniaxial tension data for SMA composites along with NiTi wire and plain fiberglass

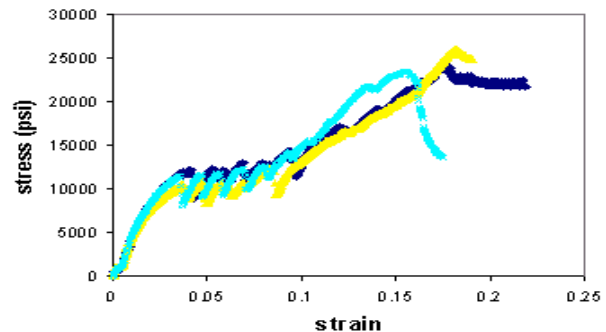


Fig. 7 Uniaxial tension data for 3 identical SMA composite specimens

Because of their increased ductility and reduced strength, the SMA composites cannot be modeled using traditional ROM formulations. Therefore, it was proposed to modify the linear ROM formulation to predict their mechanical performance. The traditional linear ROM constitutive model for a fiber reinforced composite loaded in the direction of the fibers is given as follows:

$$\sigma_{\text{composite}} = V_{\text{matrix}} \sigma_{\text{matrix}}(\epsilon_{\text{composite}}) + V_{\text{fiber}} \sigma_{\text{fiber}}(\epsilon_{\text{composite}})$$

where $\sigma_{\text{composite}}$ is the stress in the composite, $\epsilon_{\text{composite}}$ is the strain in the composite, V_{matrix} is the volume fraction of the matrix, σ_{matrix} is the stress in the matrix, V_{fiber} is the volume fraction of the fiber and σ_{fiber} is the stress in the fiber. For a fiberglass composite matrix, the stress in the matrix will be directly proportional to the stiffness of the matrix. During testing of the composites, damage in the fiberglass matrix and pullout of the NiTi wire was observed. Therefore, it was proposed to modify the linear ROM formulation by using an exponential decay of stress in the fiberglass matrix and strain transmitted to the NiTi wire as follows:

$$\sigma_{\text{matrix}} = E_{\text{matrix}} \epsilon_{\text{composite}} \exp(-\epsilon_{\text{composite}} / a)$$

$$\epsilon_{\text{composite}} = \epsilon_{\text{wire}} \exp(b \epsilon_{\text{wire}})$$

where E_{matrix} is the modulus of elasticity of the fiberglass matrix, ϵ_{wire} is the strain in the wire, and a and b are constants determined by a data fit. The results from this fit can be seen in Fig. 6 for $a = 0.045$ and $b=5$. These values provided reasonable fits to the data for all of the compositions, indicating that the deterioration in matrix strength and strain transmitted to the wires is independent of the volume fraction over the range of compositions tested.

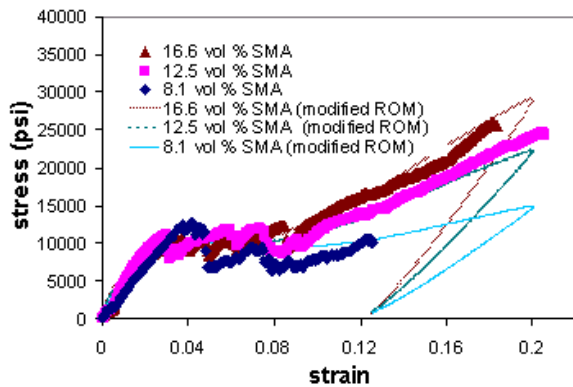


Fig.8 Modified linear ROM fits to SMA composite data

This simple constitutive model provides a computationally efficient description of material behavior to use with Finite Element Analyses for designing smart structures. Upon unloading the 0.166 volume fraction SMA composite specimens after a 20% elongation, 10% of the applied strain was recovered. This is consistent with the recovery predicted by the modified linear ROM formulation seen in Fig. 8. Because the deformation mechanisms that are

present during loading (e.g., phase transformations, damage evolution in matrix) are not active during unloading, the correlation of measured and predicted recovery strain further verifies the validity of the assumptions made in equations.

VII. ADVANTAGES AND DISADVANTAGES OF USING SHAPE MEMORY ALLOYS AS STRUCTURAL COMPOSITES

Some of the main advantages of shape memory alloys include

1. Bio-compatibility
2. Diverse Fields of Application
3. Good Mechanical Properties (strong, corrosion resistant)

There are still some difficulties with shape memory alloys that must be overcome before they can live up to their full potential. These alloys are still relatively expensive to manufacture and machine compared to other materials such as steel and aluminum. Most SMA's have poor fatigue properties; this means that while under the same loading conditions (i.e. twisting, bending, compressing) a steel component may survive for more than one hundred times more cycles than an SMA element.

VII. CONCLUSION

The functional properties of shape memory alloys offer unique opportunities in many fields of industrial activities. At present, most commercial successes are related to the use of super elasticity in biomedical applications. In near future many new commercial successes can be expected in various domains and especially in micro actuator technology and in smart materials developments. Important to notice is that the design of shape memory applications always require a specific approach, completely different from the design with structural materials.

REFERENCES

- [1] John W. Goodrum, S. Edward Law, "Rheological properties of Peanut Oil-Diesel Fuel Blends", *ASAE Transactions paper*, pp. 897-900, 2012.
- [2] C.E. Goering, A.W. Schwab, M.J. Daugherty, E.H. Pryde and A.J. Heakin, "Fuel properties of Eleven Vegetable Oils", *ASAE Transactions paper*, pp. 1472-1483, 2014.
- [3] Bhattacharya S., C.S. Reddy "Vegetable oils as fuels for Internal Combustion Engines: A Review", *Silsoe Research Institute Transaction paper*, pp. 157-165, 2017.
- [4] K. Moshizawa, K. Mori and K. Arai "Performance evaluation of non-edible vegetable oils as substitute fuels in low heat rejection diesel engines", *Proceedings of the Institution of Mechanical Engineers, paper 2000.*, Vol. 214, No. D2, pp. 181-187, 2017.
- [5] Seppo A. Niemi, Petri E. Illikainen, Mika, L.K. Makinen, Vaino and O.K. Laiho, "Performance and Exhaust Emissions of a Tractor Engine using Mustard seed oil as fuel", *SAE Transaction paper.*, 970219, pp. 21-32, 2017.
- [6] Kenton R. Kaufman, George L. Pratt and Mariusz Ziejewski Hans J. Goettler, "Fuel injection anomalies observed during Long-term Engine Performance Tests on Alternate Fuels", *SAE Transaction paper.*, 852089, pp. 591-601, 2017.

- [7] J.R. Needham and D.M. Doyle, "The combustion and Ignition Quality of Alternative Fuels in Light Duty Diesel Engine", *SAE Transaction paper*, 852101, pp. 651-671, 2017.
- [8] Dennis L. Siebers. "Ignition Delay characteristics of Alternative Diesel Fuels: Implications on cetane number", *SAE Transaction paper*, 852102, pp. 673-686.
- [9] Bernard Freedman, Marvin O. Bagby, Timothy J. Callahan and Thomas W. Ryan III "Cetane Numbers of fatty esters, Fatty alcohols and Triglycerides determined in a constant volume combustion Bomb", *SAE Transaction paper*, 900343, pp. 153-161, 2017.
- [10] Walter M. Kreucher, Weijian Han, Dennis Schuetz Zhu, Zhang Alin, Zhao Ruilan, Sun Baiming and Malcom A. Welss "Economic, Environmental and Energy Life cycle Assessment of coal conversion to Automotive Fuels in China", *SAE Transaction paper*, 982207, pp. 846-869.
- [11] R Sundara Raman, G Sankaranarayanan and N Manoharan, "Exhaust Noise Reduction Techniques in Direct Injection (D.I) Diesel Engines", *International Journal of Applied Engineering Research*, Vol. 9, No. 18, pp. 3949-3954, 2018.
- [12] R. Sundara Raman, G. Sankaranarayanan and N. Manoharan, "Smart Memory Alloys as Structural Composites", *International Journal of Applied Engineering Research*, Vol. 9, No. 18, pp. 3939-3948, 2018.
- [13] R. Sundara Raman, G. Sankaranarayanan and N. Manoharan, "Analysis of performance and emission characteristics of a diesel engine fuelled with biodiesel", *International Journal of Mechanical Engineering and Technology (IJMET)*, Vol. 6, No. 10, (Article ID: IJMET_06_10_009), pp. 66-77, 2018.
- [14] R. Sundara Raman, G. Sankaranarayanan and N. Manoharan, "Experimental Investigation on emission characteristics of a marine diesel engine with catalytic convertor for compliance with marpol regulation", *International Journal of Mechanical Engineering and Technology (IJMET)*, Vol. 6, No. 10, (Article ID: IJMET_06_10_010), pp. 78-93, 2018.
- [15] R. Sundara Raman, G. Sankaranarayanan and N. Manoharan, "Experimental Investigation on exhaust noise reduction using particulate trap in direct injection (D.I) diesel engine", *International Journal of Mechanical Engineering and Technology (IJMET)*, Vol. 6, No. 10, (Article ID: IJMET_06_10_011), pp. 94-102, 2018.